

Alumina Extraction from Red Mud by Magnetic Separation

Suprpto, Zahrotul Istiqomah, Eko Santoso, Ahmad Anwarud Dawam, and Didik Prasetyoko*

Department of Chemistry, Faculty of Science, Institut Teknologi Sepuluh Nopember, Keputih, Sukolilo, Surabaya 60111, Indonesia

Received May 19, 2017; Accepted January 10, 2018

ABSTRACT

Alumina extraction from red mud has been investigated by magnetic separation with three-step treatment. First, the addition of red mud with Na_2CO_3 (12 wt%) and heated at 110 °C for 4 h. The second step was carbon reduction using coal with mass ratio of (red mud+ Na_2CO_3) : coal was 1:3 then roasted at temperature of 850, 950, and 1050 °C for 1, 2, and 3 h. The third step was magnetic separation. The magnetic separation was carried out in order to remove magnetite produced during roasting process. Magnetic and non-magnetic phases obtained were characterized by XRD and SEM-EDX techniques. The non-magnetic phase obtained was leached using HCl 6 M, and then aluminum content was determined by Inductively Coupled Plasma (ICP). The result revealed that the highest aluminum oxide extracted from the red mud was 20.66 wt% obtained by roasting at temperature of 1050 °C for 2 h.

Keywords: red mud; magnetic separation; alumina

ABSTRAK

Ekstraksi alumina dari red mud dilakukan melalui 3 tahap perlakuan. Tahap pertama adalah penambahan Na_2CO_3 ke dalam red mud sebanyak 12% berat kemudian di oven pada 110 °C selama 4 jam. Tahap kedua reduksi karbon menggunakan batu bara yang dicampurkan ke dalam sampel tahap 1 dengan rasio (red mud + Na_2CO_3) : batu bara = 1:3, selanjutnya di kalsinasi dengan variasi suhu 850, 950, dan 1050 °C dengan variasi waktu masing-masing suhu 1, 2, dan 3 jam. Tahap ketiga adalah pemisahan secara magnetik untuk memisahkan magnetite yang terbentuk selama proses pemanasan. Fasa magnetik dan non magnetik dikarakterisasi menggunakan XRD dan SEM EDX. Selanjutnya fasa non magnetik dilindih menggunakan HCL 6 M dan dianalisis kadar aluminiumnya dengan ICP. Hasil uji ICP menunjukkan bahwa kadar alumina tertinggi adalah 20,66% berat yang diperoleh dari pemanasan pada suhu 1050 °C selama 2 jam.

Kata Kunci: red mud; pemisahan magnetik; alumina

INTRODUCTION

Red mud is waste material from the bauxite process in aluminum production. Globally, there is approximately 70 million tons of red mud produced annually. This happens because in the processing of one ton bauxite could produce approximately 0.8 to 1.5 tons of red mud [1]. Red mud is known relatively dangerous due to its high alkalinity (pH 10-12.5) [2].

Commonly, red mud contains Fe_2O_3 , Al_2O_3 , CaO, SiO_2 , TiO_2 and Na_2O [3]. The major component of red mud is Fe_2O_3 followed by Al_2O_3 . Al_2O_3 has high economic value but it must be separated beforehand from the other compounds. Nowadays, the researchers were encouraged to learn more about the process of alumina separation from red mud especially from iron oxide.

Several techniques have been developed to separate alumina from iron oxide, i.e. carbon reduction, acid leaching and magnetic separation [4]. Carbon

reduction in separation iron oxide from red mud gives alumina 0.3% [5]. Extraction by acid leaching had been reported successfully to obtain 15.13% alumina [6]. On the other hand, studies about iron oxide removal from red mud using magnetic separation obtained 10% alumina [7]. However, magnetic separation can't be carried out to remove hematite (Fe_2O_3), so that it has to be converted into magnetite (Fe_3O_4). Transformation from hematite to magnetite was conducted through roasting at temperature > 600 °C [8] while physical separation of the particles can be done by fluidization [9].

In this study the separation of alumina from red mud was conducted by the carbon reduction with temperature variation of 850, 950 and 1050 °C for 1, 2 and 3 h. After thermal process, iron oxide obtained was separated by magnetic separation, followed with leaching using hydrochloric acid.

* Corresponding author.
Email address : didikp@chem.its.ac.id

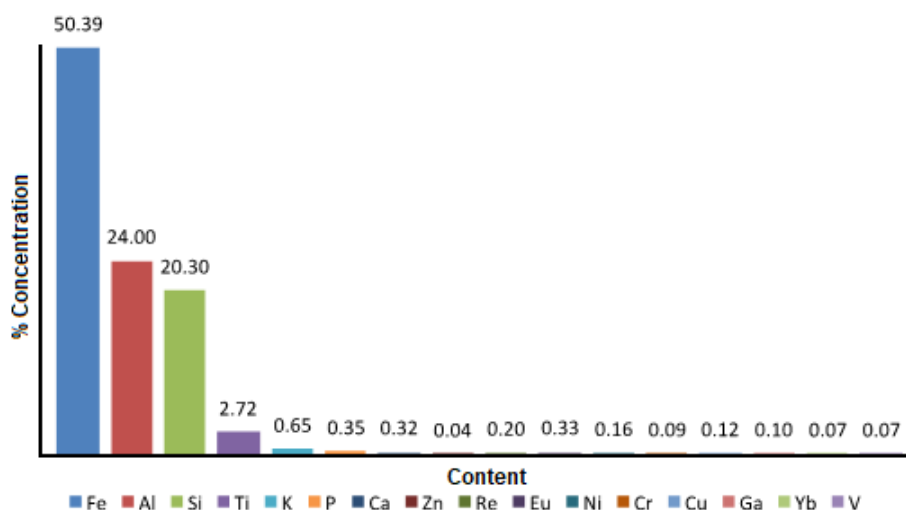


Fig 1. Content analysis of red mud by XRF

EXPERIMENTAL SECTION

Materials

The materials used in this study were red mud (from Bintan, Riau), coal, hydrochloric acid (HCl) Merck, sodium carbonate (Na_2CO_3) Merck, sodium hydroxide (NaOH) Merck and aquademine.

Instrumentation

The compositions of red mud were analyzed using X-ray Fluorescence (XRF Epsilon 1 PANanalytical). The red mud samples were characterized using X-ray Diffraction technique (XRD JOEL JDX-3530 X-ray Diffractometer) with Cu K α radiation of wavelength 1.5418 Å (40 kV and 30 mA) over the scanning range $2\theta = 2-50^\circ$. Scanning Electron Microscope (SEM) characterization was carried out using a ZEISS EVO MA 10 to monitor morphology and particle size. Electron Dispersed X-ray (EDX) (BRUKER 129 EV) was used to determine the chemical distribution of the samples. Inductively Coupled Plasma (ICP) (Prodigy) was used to measure the aluminum content in the solutions.

Procedure

Sample preparation

Red mud was crushed to obtain 74 μm particle size. The powder obtained was dried at 110 °C for 1 h to remove water content. The dried sample then characterized using XRF and XRD.

Carbon reduction of red mud

About 2 g of red mud and 0.24 g of Na_2CO_3 (12%) were mixed with aquademine, then dried at 110 °C for 4 h. Coal was added to the mixture of red mud and sodium

carbonate with ratio 1:3 (red mud + sodium carbonate : coal), then roasted at 850, 950, and 1050 °C for 1, 2, and 3 h.

Magnetic separation of iron oxide from red mud

About 0.5 g of red mud was mixed with 100 mL of aquademine and stirred for 3 h. The solid that attached to the magnetic bar was collected. Magnetic and nonmagnetic phase that obtained were dried in oven at 110 °C to remove water content and characterized using XRD and SEM-EDX.

Acid leaching of nonmagnetic phase

About 0.2 g of nonmagnetic phase was placed into conical flask then 6 M HCl was added (S/L 1: 5 g/mL). The slurry was stirred and heated at 90 °C for 2 h. The filtrate then separated from the residue by filtration. The filtrate was collected and the aluminum content was determined by ICP. 5 M NaOH solution was added slowly to the filtrate until a solution pH is 7. The precipitate that formed was collected and washed with aqua-demineralized. The precipitate obtained was dried and analyzed using ICP for its aluminum content and characterized by SEM EDX for its morphology and mineral distribution.

RESULT AND DISCUSSION

Red Mud Characterization

The composition of Bintan, Riau Island red mud was determined using XRF. The red mud composition is presented in Fig. 1. The main composition of Bintan red mud is iron while aluminum and silicone were the second and third major component. The iron content in red mud was about 50%. Thus, iron removal from red mud will

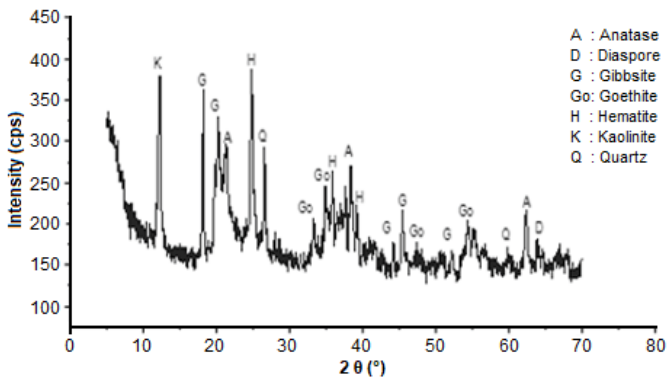


Fig 2. XRD diffractogram of red mud

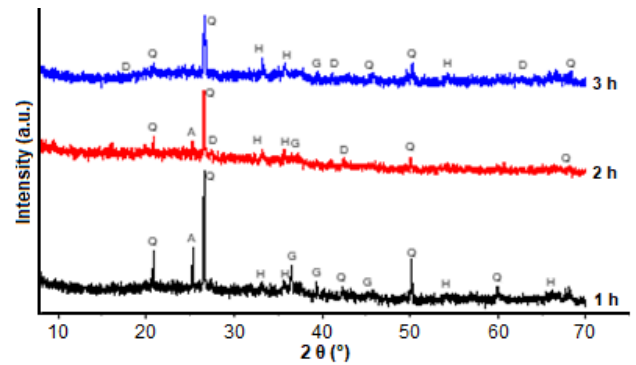


Fig 3. XRD patterns of nonmagnetic phase roasted at 850 °C

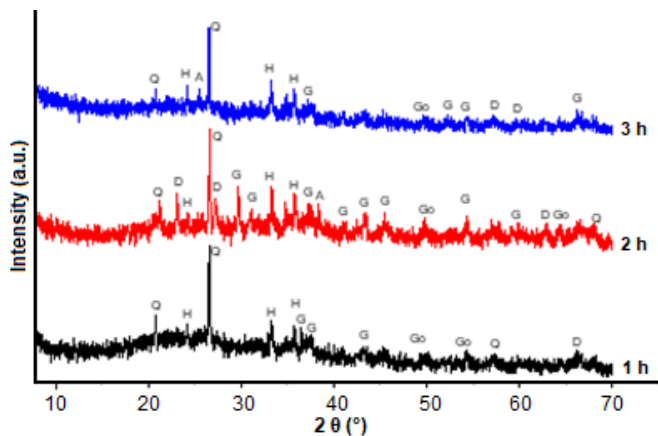


Fig 4. XRD patterns of nonmagnetic phase roasted at 950 °C

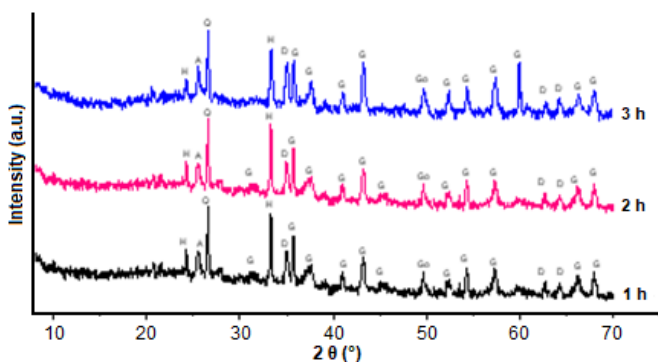


Fig 5. XRD patterns of nonmagnetic phase roasted at 1050 °C

increase the aluminum content twice of its initial concentration [10].

XRD Characterization

XRD pattern of red mud are shown in Fig. 2, there are seven minerals in the red mud that had been identified. The major component the red mud is kaolinite ($\text{Al}_2\text{Si}_2\text{O}_9\text{H}_4$) as proved by its highest main peak intensity

at $2\theta = 12.38^\circ$, while other minerals, such as hematite (Fe_2O_3), gibbsite ($\text{Al}(\text{OH})_3$), quartz (SiO_2), anatase (TiO_2), goethite (FeOOH) and diaspore (AlOOH_2) also observed.

Nonmagnetic Phase

XRD Patterns of nonmagnetic phase at roasting temperatures of 850, 950 and 1050 °C are presented in Fig. 3, 4, and 5. Quartz was the dominant phase and did not converted to other phase, while goethite transformed to hematite. Goethite would go through dehydroxylation and become hematite at temperature of 250 and 350 °C [11]. Dehydroxylation is a structural transformation that leads to structural break down of OH group. It might increase the specific surface area due to release of water that bound chemically and leads to open up goethite structure during the roasting process.

The effect of roasting time (1, 2, and 3 h) toward crystallinity of nonmagnetic phase at roasting temperature of 850 °C is shown in Fig. 3. The XRD pattern revealed that there were not any significant phase differences at varied roasting time [12]. The highest peak observed indicate that the most dominant phase was quartz. It also revealed that roasting time reduce the peak intensity of quartz and anatase as roasting time increased.

Fig. 4 shows the XRD pattern of nonmagnetic phase at roasting temperature of 950 °C (1, 2, and 3 h). It was observed that the phase were similar for each roasting time, but the peak intensity for each phase was slightly changes. Peak intensity of quartz turns out to be decreased at 950 °C compared to 850 °C, while hematite peak become pointed at 950 °C. Similar result was observed for gibbsite peaks at temperature higher than 850 °C for 2 h roasting time.

The peak of nonmagnetic phase turn out to be sharper at 1050 °C than 850 or 950 °C for roasting time 1, 2, and 3 h. XRD pattern of roasting temperature at 1050 °C (Fig. 5) shows characteristic peaks of quartz,

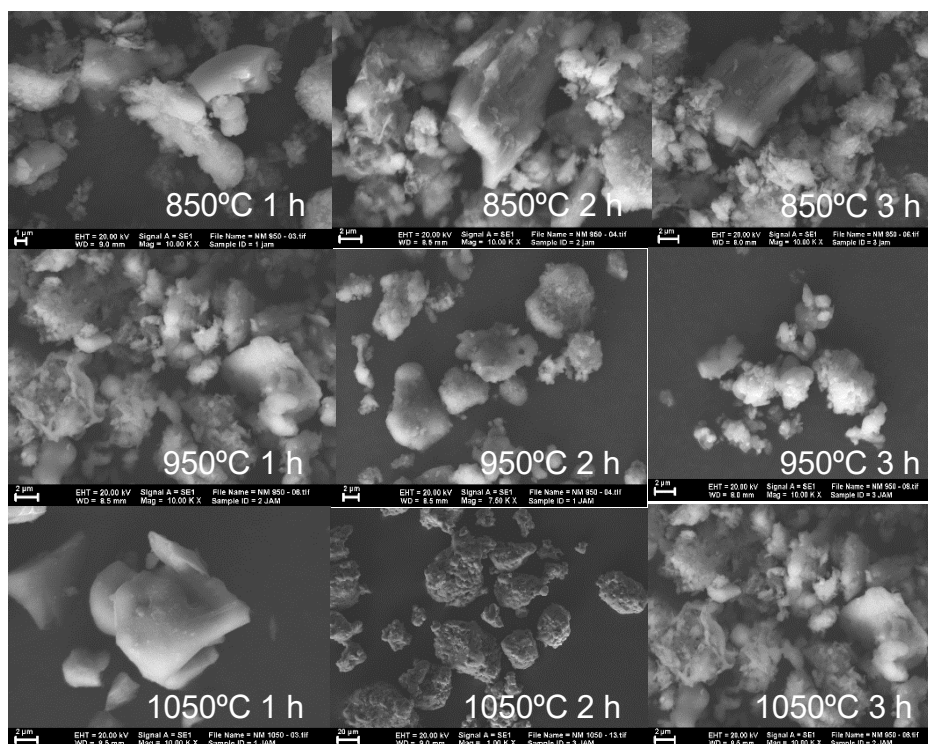


Fig 6. SEM images of nonmagnetic phase at variation roasting temperature and time

hematite, gibbsite, diaspore, and anatase. Quartz has the highest peak intensity compared to others, it indicates the dominant phase at sample was quartz. The intensity of hematite characteristic peak at 1050 °C was increased. It indicates that there was any transformation from magnetic phase to nonmagnetic phase at temperature higher than 850 °C. Crystallinity of gibbsite and anatase also turn out to be increased as temperature and roasting time increased [13].

SEM Characterization

SEM was used to characterize the morphology of nonmagnetic phase at each roasting temperature and time (Fig. 6). The morphology after roasted at 850 °C gives similar morphology for all roasting time. It was observed that agglomeration was increased as roasting time increased [14]. It was in accordance with the XRD pattern obtained that roasting time could reduce the crystallinity of sample.

Similar morphology also observed for sample that roasted at 950 °C. The existence of agglomerate with size around 10 μm was observed. The XRD pattern revealed the peak of quartz, hematite, and gibbsite.

Different morphologies observed in roasting temperature of 1050 °C. The surface morphology for 1 h roasting time was smoother than 2 h roasting time. However, sample that roasted for 2 h has porous surface, which gradually disappeared after 3 h. This phenomenon

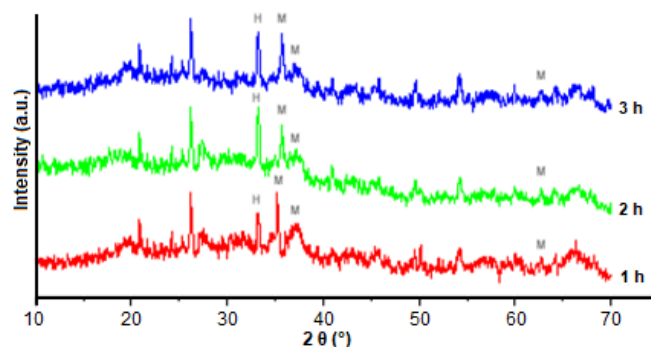


Fig 7. XRD patterns of magnetic phase roasted at 850 °C

might be caused by crystallinity alterations of gibbsite and anatase.

Magnetic Phases

XRD patterns of magnetic phase in various roasting temperature (850, 950, and 1050 °C) were shown in Fig. 7, 8, and 9. The differences between nonmagnetic and magnetic phase were observed by the existence of magnetite, Fe_3O_4 , in magnetic phase with characteristic peak at 2θ : 35, 37, 43, and 62°. Magnetite phase formation was observed at 800 °C Fig. 7, but hematite peak also appeared in magnetic phase, it indicates that hematite was not reduced completely.

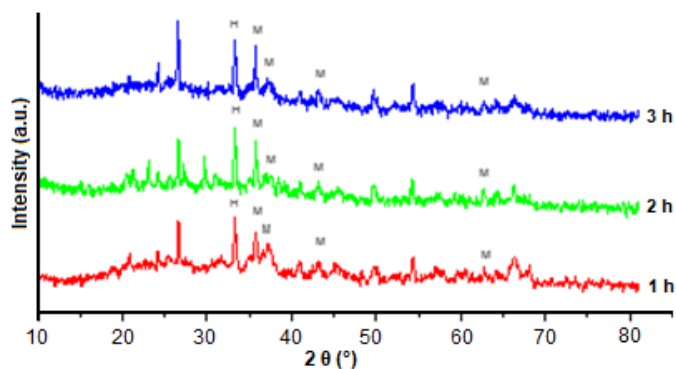


Fig 8. XRD patterns of magnetic phase roasted at 950 °C

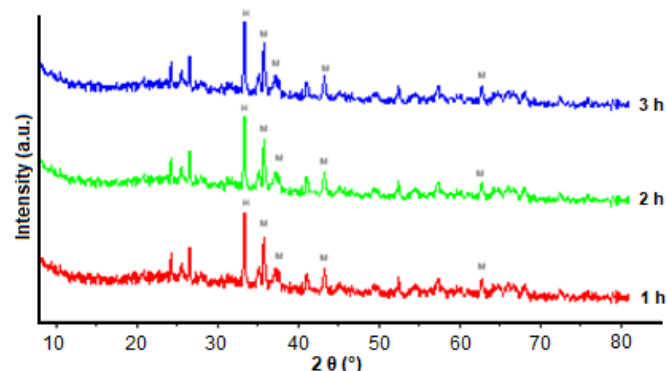


Fig 9. XRD patterns of magnetic phase roasted at 1050 °C

Table 1. Percentage of alumina extracted with different roasting temperature

No	Time (hour)	Al ₂ O ₃ (%)		
		850 (°C)	950 (°C)	1050 (°C)
1	1	12.61	14.89	15.69
2	2	17.83	19.27	20.66
3	3	15.91	15.22	12.59

Peaks at 2θ : 35, 37, and 62° were observed at roasting time for 1, 2, and 3 h. Different peak intensity was observed at roasting temperature of 950 °C for 2 h (Fig. 7). Characteristic peak of hematite turn out to be decreased while characteristic peaks of magnetic phase were increased. It indicates that roasting time could affect the phase composition of hematite and magnetite [15]. XRD pattern of magnetic phase roasted at 1050 °C (Fig. 8) has no significantly different from magnetic phase roasted at 850 and 950 °C. It indicates that hematite was converted to magnetite in all variation of roasting time and temperature.

Aluminum Leaching of Nonmagnetic Phase with HCl

Nonmagnetic phase was leached using 6 M HCl (S/L 1:5) at 90 °C for 2 h. White precipitate was obtained and separated by filtration. Because it was insoluble in HCl, the possibility of the white precipitate was silica [16]. About 5 M NaOH was added to filtrate and stirred. The solution then neutralized by addition of 6 M HCl then ICP analysis was performed to determine the aluminum concentration in the filtrate. The aluminum extracted at various roasting temperature and time are summarized in Table 1. It was observed that the highest aluminum extracted was 20.66% obtained by roasting at 1050 °C for 2 h.

CONCLUSION

Alumina extraction from red mud was successfully performed using magnetic separation. The separation

process produced two phases, magnetic and nonmagnetic phase. Nonmagnetic phase obtained was leached by hydrochloric acid, the aluminum content in the leachate was measured using ICP. The results showed that the highest aluminum extracted from the red mud sample was 20.66 wt% obtained by roasting at 1050 °C for 2 h.

ACKNOWLEDGEMENT

This research was funded by Kementerian Riset Teknologi dan Pendidikan Tinggi, Republik Indonesia.

REFERENCES

- [1] Li, G., Liu, M., Rao, M., Jiang, T., Zhuang, J., and Zhang, Y., 2014, Stepwise extraction of valuable components from red mud based on reductive roasting with sodium salts, *J. Hazard. Mater.*, 280, 774–780.
- [2] Zhong, L., Zhang, Y., and Zhang, Y., 2009, Extraction of alumina and sodium oxide from red mud by a mild hydro-chemical process, *J. Hazard. Mater.*, 172 (2-3), 1629–1634.
- [3] Li, X., Wei, X., Wei, L., Liu, G., Peng, Z., Zhou, Q., and Qi, T., 2009, Recovery of alumina and ferric oxide from bayer red mud rich in iron by reduction sintering, *Trans. Nonferrous Met. Soc. China*, 19 (5), 1342–1347.
- [4] Liu, Y., and Naidu, R., 2014, Hidden values in bauxite residue (red mud): Recovery of metals, *Waste Manage.*, 34 (12), 2662–2673.
- [5] Raspopov, N., Korneev, V., Averin, V., Lainer, Y.A., Zinovev, D., and Dyubanov, V., 2013, Reduction of iron oxides during the pyrometallurgical processing of red mud, *Russ. Metall.*, 2013 (1), 33–37.
- [6] Cengeloglu, Y., Kir, E., Ersoz, M., Buyukerkek, T., and Gezgin, S., 2003, Recovery and concentration of metals from red mud by donnan dialysis, *Colloids*

- Surf.*, A, 223 (1-3), 95–101.
- [7] Li, Y., Wang, J., Wang, X., Wang, B., and Luan, Z., 2011, Feasibility study of iron mineral separation from red mud by high gradient superconducting magnetic separation, *Physica C*, 471 (3-4), 91–96.
- [8] Liu, Y., Zhao, B., Tang, Y., Wan, P., Chen, Y., and Lv, Z., 2014, Recycling of iron from red mud by magnetic separation after co-roasting with pyrite, *Thermochim. Acta*, 588, 11–15.
- [9] Sahoo, P., and Sahoo, A., 2014, Hydrodynamic studies on fluidization of red mud: CFD simulation, *Adv. Powder Technol.*, 25 (6), 1699–1708.
- [10] Jamieson, E., Jones, A., Cooling, D., and Stockton, N., 2006, Magnetic separation of Red Sand to produce value, *Miner. Eng.*, 19 (15), 1603–1605.
- [11] Tang, H., Sun, W., Hu, Y., and Han, H., 2016, Comprehensive recovery of the components of ferritungstite base on reductive roasting with mixed sodium salts, water leaching and magnetic separation, *Miner. Eng.*, 86, 34–42.
- [12] Zhu, D., Chun, T., Pan, J., and He, Z., 2012, Recovery of iron from high-iron red mud by reduction roasting with adding sodium salt, *J. Iron Steel Res. Int.*, 19 (8), 1–5.
- [13] Ramdhani, E.P., Wahyuni, T., Ni'mah, Y.L., Suprpto, S., and Prasetyoko, D., Extraction of alumina from red mud for synthesis of mesoporous alumina by adding CTABr as mesoporous directing agent, *Indones. J. Chem.*, In Press.
- [14] Samouhos, M., Taxiarchou, M., Pilatos, G., Tsakiridis, P.E., Devlin, E., and Pissas, M., 2017, Controlled reduction of red mud by H₂ followed by magnetic separation, *Miner. Eng.*, 105, 36–43.
- [15] Sun, Y., Han, Y., Gao, P., Wang, Z., and Ren, D., 2013, Recovery of iron from high phosphorus oolitic iron ore using coal-based reduction followed by magnetic separation, *Int. J. Miner. Metall. Mater.*, 20 (5), 411–419.
- [16] Widiyati, C., and Poernomo, H., 2005, Stabilization of dry sludge of liquid waste of leather treatment by using fly ash, *Indones. J. Chem.*, 5 (1), 36–40.